Room-temperature reduction at $SrRuO_3$-metal interface in hydrogenous atmosphere detected by interface-sensitive resistance measurement

Hiroshi Kambara,[1, a)] Hiroyuki Tanaka,[1] Satoru Oishi,[1] Kenichi Tenya,[1] and Hiroyuki Tsujii[2]

[1)] *Department of Physics, Faculty of Education, Shinshu University, Nagano 380-8544, Japan*

[2)] *Department of Physics, Faculty of Education, Kanazawa University, Kanazawa 920-1192, Japan*

Using interface-sensitive resistance measurement techniques, we detected the reducing reaction precursor at the interface between the metallic oxide $SrRuO_3$ and the electrodes under a hydrogenous atmosphere at room temperature. The interface resistance between this polycrystalline oxide and the electrodes (metallic pads or wires) clearly increased with the hydrogen present even at room temperature. In contrast, for bulk $SrRuO_3$, no increase in resistance was found. The rate of increase of the interface resistance depends on the electrode material. For example, that of $SrRuO_3$-Ag is larger than that of $SrRuO_3$-Cu, and the rate is related to the propensity for bulk oxide to reduce; Ag_2O is easier to reduce than CuO. The origin of the increase in interface resistance is posited to be the partial deficiency of oxygen in $SrRuO_3$. Our experiments suggest that the reduction at the interface of $SrRuO_3$ occurs at relatively low temperatures (room temperature) compared with the bulk reducing temperature of ~ 200°C previously reported. In addition, electrode materials control the reducing reaction at the interface.

[a)] kambara@shinshu-u.ac.jp

I. INTRODUCTION

Hydrogen causes drastic changes in matter. For example, atomic hydrogen adsorbed on insulating $SrTiO_3$ induces a metallic state at the surface[1]. Very recently, extreme high-temperature superconductivity was discovered in high-pressurized hydrogen compounds; specifically, H_3S at 203 K[2], and LaH_{10} at 250 K[3]. Not only for basic science but also for applied science, hydrogen attracts much attention because of its great potential as an extremely clean energy source without producing CO_2. To date, the high number of studies attest to the variety of fields delving into hydrogen-related science. Although reduction is one of the simplest chemical reactions, the reaction is usually performed at higher temperatures than room temperature because the thermal energy usually accelerates the chemical reaction. For instance, the reduction of CuO is not expected at room temperature without heating. In general, because the surface/interface state is qualitatively different from the bulk state, the reducing reaction temperature at the surface/interface is different from the bulk. Therefore, bulk and surface/interface reactions must be assessed separately.

The $SrRuO_3$ (SRO) oxide is one of the rare electrically conducting oxides without doping and exhibits a rather high conductivity[4,5]. The bulk properties have been well studied, especially the ferromagnetic transition, which occurs at 160 K[4,5]. Owing to its pseudo cubic perovskite structure and good lattice matching to other perovskite oxides, SRO is used in applications as an electrode in functional devices[5]. However, SRO films degrade and become less conductive in forming gas (FG, e.g. 5% H_2 + 95% Ar) annealing, which is necessary to improve the quality of Si-based devices. According to Halley and colleagues[6], the resistivity of a SRO film starts to increase at $\sim$ 300°C because of hydrogen diffusion and rapidly changes at $\sim$ 500°C through the decomposition of SRO during FG annealing; corresponding in-situ X-ray diffraction (XRD) signals at $\sim$ 200°C and at $\sim$ 450°C were also observed. From XRD measurements, Lin and colleagues[7,8] reported the degradation of SRO films starting at $\sim$ 200°C in the FG (3% H_2 + 97% N_2) annealing process. From a thermogravimetry analysis, Mlynarczyk and colleagues[9] observed a loss of sample mass at 300°C during FG (4% H_2 + 96% Ar) annealing, whereas from thermochemical reactivity measurements in flowing molecular hydrogen, Bensch and colleagues[10] reported an onset temperature of 800 K ($\sim$ 530°C) in the reduction of SRO single crystals. All previous experiments had been done with SRO films or crystals; whether reducing reactions simultaneously occurred in the

bulk and at the surface/interface was not necessarily clear.

Here, from electrical transport measurements, we report room-temperature reduction at the interface of a ruthenium oxide compound. We adopted separately bulk and interface-sensitive resistance measurement techniques, and measured both the bulk and interface resistances of SRO in a hydrogen atmosphere at room temperature. We emphasize again that the room temperature is much lower than the onset temperature of decomposition ~ 200°C that was previously reported[6–8].

II. EXPERIMENTAL METHODS

The main samples of polycrystalline SRO were prepared using a conventional solid-state reaction method with $SrCO_3$ and RuO_2 as starting materials. After careful mixing, the materials were shaped into pellets and sintered at 1100°C in air. After crushing the pellets, the above process was then repeated. Typically, the range of grain sizes of sintered SRO is approximately 0.1–1 μm, which we obtained from scanning electron microscope images[11]. The pellets were cut into thin slabs ($\sim 3 \times 2 \times 0.5$ mm^3) for resistance measurements.

Electrical resistances were measured using three methods: (i) four-terminal (4T) sensing for the bulk sample, (ii) three-terminal (3T) sensing for the interface between sample and conductive epoxy pad, and (iii) point-contact (PC) for the interface between sample and metallic wire tip. Each of these methods have specific features, which we outline separately in the above order:

(i) For the 4T method, the conventional technique, the two current-supply lines are isolated from the two voltage-measurement lines so as not to measure the interface resistance between sample and conductive epoxy pads [see Fig. 1(a)].

(ii) For the 3T method, one of the two conductive epoxy pads for the current lines is common to one of those for the voltage lines [Fig. 1(b)]. Thus, the interface resistance between sample and conductive epoxy pad is measured [see circuit diagram at the bottom of Fig. 1(b)]. Note that the 3T method is sensitive to the interface resistance and not the bulk. Hereafter, without further notice, we used Ag epoxy for the pads except for the SRO 3T measurements, for which we used both Ag and Cu epoxy to check the influence of different materials. For the 4T and 3T methods, we measured not only the SRO samples but also samples of commercial Pd (purity 99.95%), Cu (purity 99.96%), and sintered carbon

composition resistors (2.2 Ω); they are used as references, namely, a hydrogen-storing metal, a non-hydrogen-storing metal, and a porous material, in the above same order. Furthermore, concerning the 3T method, we measured sintered RuO_2 polycrystalline samples. The RuO_2 samples, which were made of commercial RuO_2 powder sintered at 1050°C with oxygen gas flow, showed good metallic behavior similarly to SRO as the temperature decreased.

(iii) For the PC method, a metallic tip is pushed gently against the sample surface to form the junction. The junction resistance is usually much larger than the bulk resistance of the sample or the metallic tip itself. Therefore, the PC measurement is also sensitive to the sample-tip interface. We used five different commercial metallic wires (0.20 mm in diameter) for the tips: Au (purity 99.95%), Pt (purity 99.98%), Ag (purity 99.99%), Cu (purity 99.9%), and Fe (purity 99.5%).

The experimental measurements were taken following a set procedure. First, to evaluate the initial states, 4T or 3T resistance−temperature (R–T) measurements for the initial samples (not exposed to hydrogen gas) were performed in vacuum ($< 1 \times 10^{-3}$ Pa), using a Gifford–McMahon refrigerator, over a cooling and warming cycle from room temperature to 4 K and then back to room temperature. Next, at room temperature, under a pressure of 3.5×10^4 Pa, hydrogen gas (commercial composition of purity 99.999%) was fed into the vacuum chamber exposing the samples to hydrogen molecules for a duration of two days. During this exposure, the time variation of the resistance $R(t)$ was measured in the closed chamber. Then, after pumping the hydrogen gas out, the 4T or 3T R–T measurements were performed again in vacuum for the hydrogen-exposed samples. Moreover, $R(t)$ for the 3T SRO samples were obtained not only at room temperature but also higher temperatures (between 30–60°C), which were regulated using a mantle heater surrounding the chamber. For the PC method, however, a freshly nipper-cut metallic wire tip was set closely to the SRO sample surface in the vacuum chamber. After pumping the ambient air out from the chamber to less than 1×10^{-3} Pa, the tip was pushed gently against the sample surface to form the SRO-tip interface. At the regulated temperatures up to 60°C (as for the 3T SRO measurements), the interface resistance remained stable. Hydrogen gas at a pressure of 3.5×10^4 Pa was again established in the chamber, and $R(t)$ variations of the samples were measured over two days. The R–T measurements for the 4T and 3T methods were performed using the standard lock-in technique applying an ac modulation frequency of 89.3 Hz. On the other hand, $R(t)$ measurements in hydrogenous atmosphere at room temperature

or regulated temperatures up to 60°C for 4T, 3T and PC methods were performed using either this lock-in technique or the dc method using a Keithley 2400 source-measure unit.

III. RESULTS

Figure 2(a,b) shows the R–T results for Pd and SRO, respectively, obtained from the 4T method before and after hydrogen exposure. For Pd, the resistance after hydrogen exposure becomes higher than that before exposure and features an anomaly around 50 K. This anomaly is strong evidence that hydrogen atoms dissolve into the palladium lattice sites through the glass transition[12–14]. In contrast, the 4T R–T of SRO [Fig. 2(b)] shows no changes when exposed to hydrogen. The curves appear the same and feature a kink at 160 K that arises from the ferromagnetic transition for both samples, indicating that hydrogen neither dissolves into the SRO lattice nor affects this transition. Next, the 3T R–T curve of the data for Pd after hydrogen exposure [Fig. 2(c)] is similar to that before exposure, except that the resistances are higher after hydrogen exposure than before exposure. We recall that the 3T method yields not the bulk but the interface resistance, the latter being approximately a hundred times larger than the former. Similar to the Pd result, the two 3T R–T curves for SRO before and after hydrogen exposure [Fig. 2(d)] are similar in shape and resistances are higher after hydrogen exposure than before. This higher resistance after hydrogen exposure is evidence of a hydrogen reaction at the SRO interface because, from the 4T curves [Fig. 2(b)], the bulk resistance shows no change after hydrogen exposure. In addition, the 3T resistances for SRO are approximately 30 times larger than those obtained from the 4T method, indicating that the 3T data reflect not the bulk but the interface resistance. We also note that the ferromagnetic transition kink at 160 K becomes dull for 3T R–T [Fig. 2(d)] compared with the 4T curve [Fig. 2(b)] probably because the ferromagnetic transition is suppressed at the interface.

Figure 3 shows the $R(t)$ results obtained using the 4T and 3T methods for SRO, Pd, Cu, and C at room temperature. Here we compare the normalized resistance $R(t)/R_0$, where R_0 is the resistance just after introducing hydrogen into the chamber. Whereas the absolute value of R depends on the width of the epoxy pad, the normalized $R(t)/R_0$ is free from such experimental uncertainties. We examined $R(t)/R_0$ for two different 3T SRO samples with different R_0 values with both yielding almost identical curves (not shown here). Initially,

the hydrogen response to the resistance of 4T method was only detected in Pd, whereas no response was detected in SRO, Cu, and C. The 4T resistance of Pd immediately starts to increase just after hydrogen exposure reaching a saturated value after 10 h had passed. The bulk resistance of PdH_x is known to monotonically increase as x increases from 0 to 0.75[15]. This result shows that only Pd stores hydrogen inside the bulk material, whereas the others do not. Next, for the 3T $R(t)$ measurements, we see the resistance increases for SRO as well as Pd, whereas Cu and C do not show significant increases. Here, we note that $R(t)/R_0$ of SRO started to increase just after hydrogen exposure whereas for Pd there was some delay in the rise of $R(t)/R_0$. Furthermore, $R(t)/R_0$ of SRO continued to increase for two days and did not show any saturation behavior; for Pd, a saturated value was reached after 20 h. These results show that SRO reacts immediately with hydrogen at the interface and continues for a long time. In contrast, Pd reacts with hydrogen first inside the bulk and subsequently at the interface, and finished reacting, although the reason for the delay in starting at the interface is unclear. Therefore, the increase in $R(t)/R_0$ for SRO is qualitatively different from that for Pd.

The temperature dependence of $R(t)/R_0$ for SRO obtained from the 3T method [Fig. 4(a)] shows that the increase in $R(t)/R_0$ is larger with higher temperatures, suggesting that the hydrogen reaction at the interface is thermally activated. Here, we note that above 303 K the data were taken at regulated temperatures controlled by a mantle heater. The data below 299K were taken at unregulated temperatures, although an average temperature with a slight fluctuation ($\pm \sim 1$ K) was obtained. In addition, the upper limit for this experimental setup was 333 K and was imposed to avoid thermal leaks caused by thermal expansion from the taper-sealed vacuum chamber. The behavior for data at 318 K, after the hydrogen exposure experiment, is also shown: from 47 h to 58 h, hydrogen gas was pumped out using a turbo molecular pump and afterwards fresh air was introduced into the chamber at atmospheric pressure. Interestingly, on substituting hydrogen for fresh air, the interface resistance decreased. We believe that oxygen atoms in the air play an important role to recover electrical conductivity at the interface; this role is discussed later. Figure 4(b) shows a plot of $\Delta R(t)/R_0$ versus temperature, where $\Delta R(t)/R_0 = R(t)/R_0 - R(0\,\mathrm{h})/R_0 = R(t)/R_0 - 1$ is the normalized resistance increase from 0 h to t (here, we show $t = 10$ h and 40 h). From an approximate extrapolation, we expect a non-zero $\Delta R(t)/R_0$ to be observed at approximately $270 \sim 280$ K. This result suggests that the hydrogen reaction occurs at

the SRO interface at ~ 0°C, which is much lower than the bulk reducing temperature of ~ 200°C[6–8].

In Fig. 5(a), we show the 3T $R(t)/R_0$ result for RuO_2 at 303 K compared with the SRO result obtained under the same experimental conditions. We observed an increase in 3T $R(t)/R_0$ at the RuO_2 interface similar to SRO at room temperature, although the rate of increase is smaller than that of SRO. Figure 5(b) shows the epoxy material dependence of 3T $R(t)/R_0$ for SRO. With Cu-epoxy pads, the increase in $R(t)/R_0$ during hydrogen exposure is much less than for the Ag-epoxy pads. This result suggests that rate of hydrogen reaction depends on the epoxy material.

To check the influence of the contact materials, we performed several PC experiments (see Figs. 6 and 7). As tips, we used five wires of different metals, specifically, Au, Pt, Ag, Cu, and Fe. Each metal tip was pushed gently against the SRO surface to form a junction (see lower inset of Fig. 7), the resistance of which is typically $\sim 1\ \Omega$ (Fig. 6). We used two different tips of the same metal with different pushing strengths, for which R_0 are different by a factor of ~ 2. Just after hydrogen exposure, an unexpected jump in R sometimes occurs that arises through some vibrational instability during the feeding of the hydrogen gas. To remove the uncertainty, we defined R_0 as the resistance just after the jump from which the resistance starts gradually to increase (Fig. 6). Figure 6 shows the qualitative similarity of trends in $R(t)/R_0$ for the same metal. Although the increasing magnitude in $R(t)/R_0$ of Ag is different from each other, the other materials (for Au and Cu, in especial) show good reproducibility in $R(t)/R_0$. Figure 7 shows the tip material dependence of $R(t)/R_0$. Here, we chose the data of Ag#1 (see Fig. 6) for Ag because of the following reasons. Empirically, we studied that successive hydrogen exposure enhanced the increase in $R(t)/R_0$ for the PC experiments (not shown here) probably because of the progress of the interface degradation. If surface degradation might exist before hydrogen exposure, a large increase in $R(t)/R_0$ might occur despite the initial hydrogen exposure, as seen in the case of Ag#2. In Fig. 7, we see that rate of increase in $R(t)/R_0$ depends on the material. Within ~ 5 h, the data of $R(t)/R_0$ for Au and Pt show almost identical curves and feature the largest changes among the five materials. Concerning for Ag, Cu, and Fe, the increases become smaller in magnitude. We note that the rate of reaction is larger for Ag than Cu, which is in qualitative agreement with earlier results [Fig. 5(b)]. Beyond ~ 10 h, for all materials except Cu, the increase in $R(t)/R_0$ gradually slows. For the Cu-tip, the increase is monotonic (Fig. 7,

upper inset). Here, we note that the tip hardness of the material is not a critical factor of the PC experiments because no correlation in Mohs scale is found; specifically, 2.5–3 (Au), 4.3 (Pt), 2.5 (Ag), 3 (Cu), 4.5 (Fe). Here, each numerical value denotes the Mohs scale. That is, if we divide the five different tips into two groups of similar hardness, specifically (Au, Ag, Cu) and (Pt, Fe), common trends are not observed.

In Fig. 8, we compare the resistance increase normalized to that from 0 to 5 h, $\Delta R(t)/\Delta R(5\,\mathrm{h}) = (R(t) - R_0)/(R(5\,\mathrm{h}) - R_0)$, obtained by the different methods—3T and PC for Ag and Cu [see Figs. 5(b) and 7]. The normalized data of Ag-epoxy (3T) and Ag-tip (PC) show a remarkable similarity in time dependence. In contrast, the two curves for Cu show a linear time dependence, which is qualitatively different from that for Ag although the two Cu curves are not equivalent. Therefore, we assert that electrode material dependence of hydrogen reaction is not trivial but intrinsic.

IV. DISCUSSION

We summarize the important results from our SRO experiments: (1) The 3T $R(t)/R_0$ results show a continuous increase in resistance during hydrogen exposure even at room temperature; in contrast, the 4T results do not. (2) The rates of increase in 3T $R(t)/R_0$ are larger at higher temperatures. (3) The rates of increase in 3T $R(t)/R_0$ depend on the conducting epoxy materials being larger with Ag epoxy pads than with Cu ones. (4) In regard to (3), the rates of increase in the PC $R(t)/R_0$ depend on the tip material, being largest for Au and Pt tips, then, Ag, Cu, and smallest for Fe.

Considering these results, we discuss the origin of the increase in resistance at the SRO-metal interface. According to Halley and colleagues[6], with the FG annealing of SRO, weak and smooth increases in resistivity were observed at ~ 300°C because of hydrogen diffusing into the SRO lattice and the generation of oxygen vacancies: $SrRuO_3 + xH_2 \rightarrow SrRuO_{3-x} + xH_2O$. Further heating to ~ 500°C showed a sharp transition in resistivity because of the decomposition of SRO: $SrRuO_3 + 2H_2 \rightarrow SrO + Ru + 2H_2O$. Therefore, at ~ 300°C, the conducting network ($\cdots$-O-Ru-O-$\cdots$) starts to break up, and the resistance increases gradually. Next, agglomerating islands of Ru generated at ~ 500°C are isolated from the conducting network, and the resistance rapidly increases[10]. Here, we also note that the SRO resistivity was observed to increase and change from a metallic behavior to a semi-

conducting behavior under a reduced oxygen pressure during film growth[16]. Hence, oxygen deficiency certainly lowers the conductivity in SRO.

With the room temperature being much lower than the bulk reducing temperature, the resistance of the bulk most likely never changes under a hydrogen atmosphere at room temperature. In this work, however, we suggest that a partial reduction (oxygen deficiency) occurs at the interface even at room temperature for the following reasons. Concerning result (2), the hydrogen reducing reaction conceivably had accelerated at higher temperatures. Furthermore, the recovery of conductivity for hydrogen-exposed SRO samples through the exposure to fresh air [Fig. 4(a)] implies an opposite reaction to a reduction. Plausibly, oxidation, which repairs oxygen vacant networks in $SrRuO_{3-x}$-metal channels, recovers the conductivity at the interface. Here, we note that air contains not only O_2 but also N_2, H_2O, and other gases. However, N_2 should be inactive and H_2O reacts with SrO to form $Sr(OH)_2$, which results in a degradation of the SRO interface[8] that involves the reverse reaction that decreases the resistance. Thus, we regard O_2 as a key molecule in recovering electrical conductivity. Regarding results (3) and (4), an Ellingham diagram[17], which represents the Gibbs free energy versus temperature to form metal oxides, is considered and shows reducing trends for several metal oxides. For example, bulk Ag_2O is easily reduced by heating to only 200°C without a reducing agent, whereas CuO is hard to reduce without a reducing agent and heating to 1800°C is needed. Furthermore, FeO is harder to reduce than CuO. Therefore, the most stable material to use in a reducing environment among FeO, CuO, and Ag_2O is FeO, the next being CuO, and the last Ag_2O. We speculate that the initial rate of increase in $R(t)/R_0$ is closely related with the reducing trends of the electrode material oxides. Here, we assume pseudo-oxides based on Ag, Cu, and Fe form at the interface of the SRO because of overlaps of their wave functions (Fig. 9). Because Ag_2O is easier to reduce than CuO, the rate of increase in $R(t)/R_0$ for an Ag epoxy pad/tip is likely to be larger than that of Cu. In light of this work, there is consistency with this scenario in that the rate of increase of $R(t)/R_0$ for Fe is the smallest. In contrast, Au and Pt hardly form oxides. Therefore, in this instance, oxygen atoms at the interface are easily reduced with hydrogen because Au(Pt)-O bonding is weak. Then, the rate of increase in $R(t)/R_0$ for Au and Pt are similar and are largest among Au, Pt, Ag, Cu, and Fe.

From recent surface XRD experiments for $RuO_2(110)$ on Ru(0001), the XRD signals show a partial reduction on the RuO_2 surface following hydrogen exposure (1.1×10^{-5} Pa of H_2)

even at 300 K[18]. This report supports our scenario of a room-temperature reduction at the SRO-metal interface. In Fig. 5(a), we observed that the rate of increase in 3T $R(t)/R_0$ for RuO_2 is smaller than that of SRO. The origin of the quantitative difference is as yet unclear, however, the existence of SrO as well as RuO_2 in SRO may affect the reducing rate and should be resolved in the near future.

As an additional remark, if H_2O is generated as a result of reduction, it may subsequently react with SrO to form $Sr(OH)_2$[8]. In this case, because $R(t)/R_0$ has also a tendency to increase from losses in the conducting network, distinguishing them as originating from a reduction only or a water reaction in addition is difficult at present.

V. CONCLUSIONS

Using separately the interface and bulk-sensitive measurement techniques of electrical resistance, we studied the reducing reaction for conducting ruthenium oxide $SrRuO_3$ in a hydrogen environment near room temperature. We found that the room-temperature interface-sensitive resistance between $SrRuO_3$ and a pad/tip of a metal electrode increases in a reducing environment, whereas no variation in resistance is seen for the bulk. We conclude that the partial reduction occurs at the $SrRuO_3$-metal interface even at room temperature and is much lower than the bulk reducing temperature. We also found that the reducing rates depend on the stability of the metal oxides present in the electrode against the reducing environment; that is, the rate of reaction is higher in more unstable oxides.

ACKNOWLEDGMENTS

The authors are grateful to T. Kawae for fruitful discussions. This work was supported by JSPS KAKENHI Grant Number JP19K03743. We thank Richard Haase, Ph.D, from Liwen Bianji, Edanz Group China (www.liwenbianji.cn/ac), for editing the English text of a draft of this manuscript.

DATA AVAILABILITY

The data that support the findings of this study are available from the corresponding author upon reasonable request.

REFERENCES

[1]M. D' Angelo, R. Yukawa, K. Ozawa, S. Yamamoto, T. Hirahara, S. Hasegawa, M. G. Silly, F. Sirotti, and I. Matsuda, Phys. Rev. Lett. **108**, 116802 (2012).

[2]A. P. Drozdov, M. I. Eremets, I. A. Troyan, V. Ksenofontov, and S. I. Shylin, Nature **525**, 73 (2015).

[3]A. P. Drozdov, P. P. Kong, V. S. Minkov, S. P. Besedin, M. A. Kuzovnikov, S. Mozaffari, L. Balicas, F. F. Balakirev, D. E. Graf, V. B. Prakapenka, E. Greenberg, D. A. Knyazev, M. Tkacz, and M. I. Eremets, Nature **569**, 528 (2019).

[4]P. B. Allen, H. Berger, O. Chauvet, L. Forro, T. Jarlborg, A. Junod, B. Revaz, and G. Santi, Phys. Rev. B **53**, 4393 (1996).

[5]G. Koster, L. Klein, W. Siemons, G. Rijnders, J. S. Dodge, C.-B. Eom, D. H. A. Blank, and M. R. Beasley, Rev. Mod. Phys. **84**, 253 (2012).

[6]D. Halley, C. Rossel, D. Widmer, H. Wolf, and S. Gariglio, Mat. Sci. Eng. B **109**, 113 (2004).

[7]J. Lin, K. Natori, Y. Fukuzumi, M. Izuha, K. Tsunoda, K. Eguchi, K. Hieda, and D. Matsunaga, App. Phys. Lett. **76**, 2430 (2000).

[8]J. Lin, K. Tsunoda, K. Eguchi, K. Hieda, and D. Matsunaga, J. Vac. Sci. Technol. A **20**, 84 (2002).

[9]M. Mlynarczyk, K. Szot, A. Petraru, U. Poppe, U. Breuer, R. Waser, and K. Tomala, J. App. Phys. **101**, 023701 (2007).

[10]W. Bensch, H. W. Schmalle, and A. Reller, Sol. Sta. Ion. **43**, 171 (1990).

[11]H. Kambara, Y. Obinata, K. Tenya, and H. Tsujii, Jpn. J. App. Phys. **55**, 093004 (2016).

[12]P. Vajda, J. P. Burger, J. N. Daou, and A. Lucasson, Phys. Rev. B **33**, 2286 (1986).

[13]K. Yamakawa, J. Alloys Compd. **393**, 70 (2005).

[14]H. Akiba, H. Kobayashi, H. Kitagawa, M. Kofu, and O. Yamamuro, Phys. Rev. B **92**, 064202 (2015).

[15]Y. Sakamoto, K. Takai, I. Takashima, and M. Imada, J. Phys.: Cond. Matt. **8**, 3399 (1996).

[16]M. Hiratani, C. Okazaki, K. Imagawa, and K. Takagi, J. J. App. Phys. **35**, 6212 (1996).

[17]P. Atkins, T. Overton, J. Rourke, M. Weller, and F. Armstrong, *Shriver and Atkins' Inorganic Chemistry, fifth ed.* (Oxford University Press, 2010) Chap. 5.

[18]H. Over, Chem. Rev. **112**, 3356 (2012).

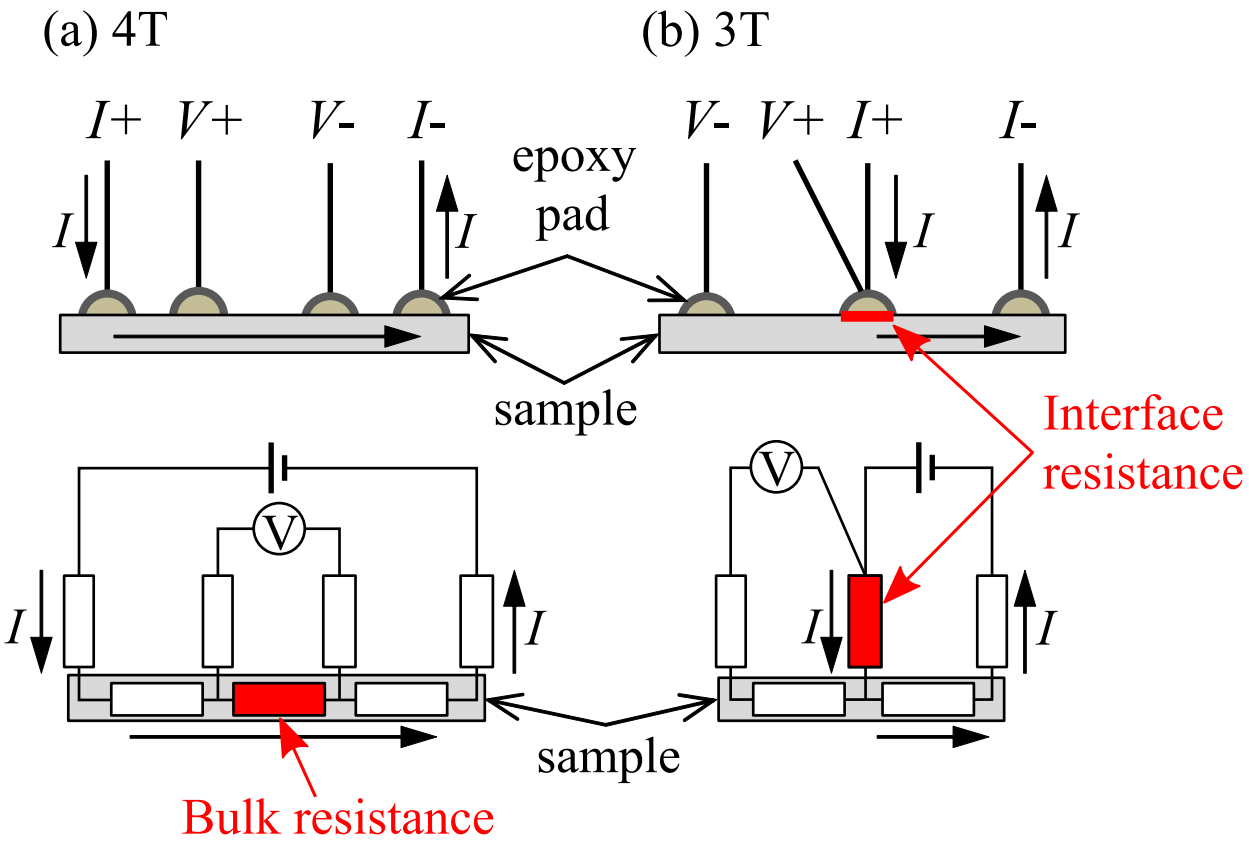

FIG. 1. Schematics of the wiring (upper) and circuit diagrams (lower) of the electrical resistance measurements for (a) four terminal (4T) and (b) three terminal (3T) methods. Each method measures the resistances marked in red.

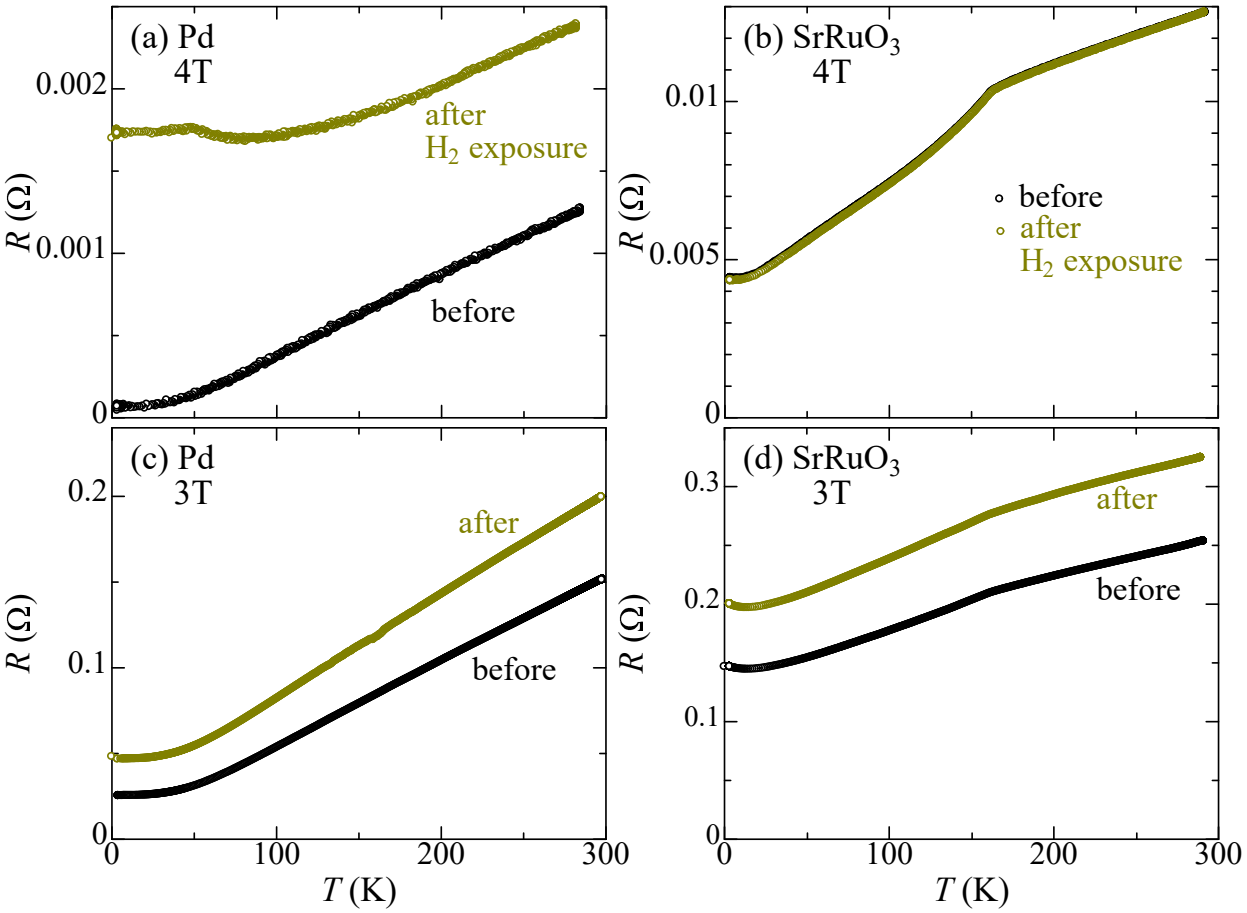

FIG. 2. R–T data for (a) Pd 4T, (b) $SrRuO_3$ 4T, (c) Pd 3T, and (d) $SrRuO_3$ 3T taken during cooling before and after H_2 gas exposure.

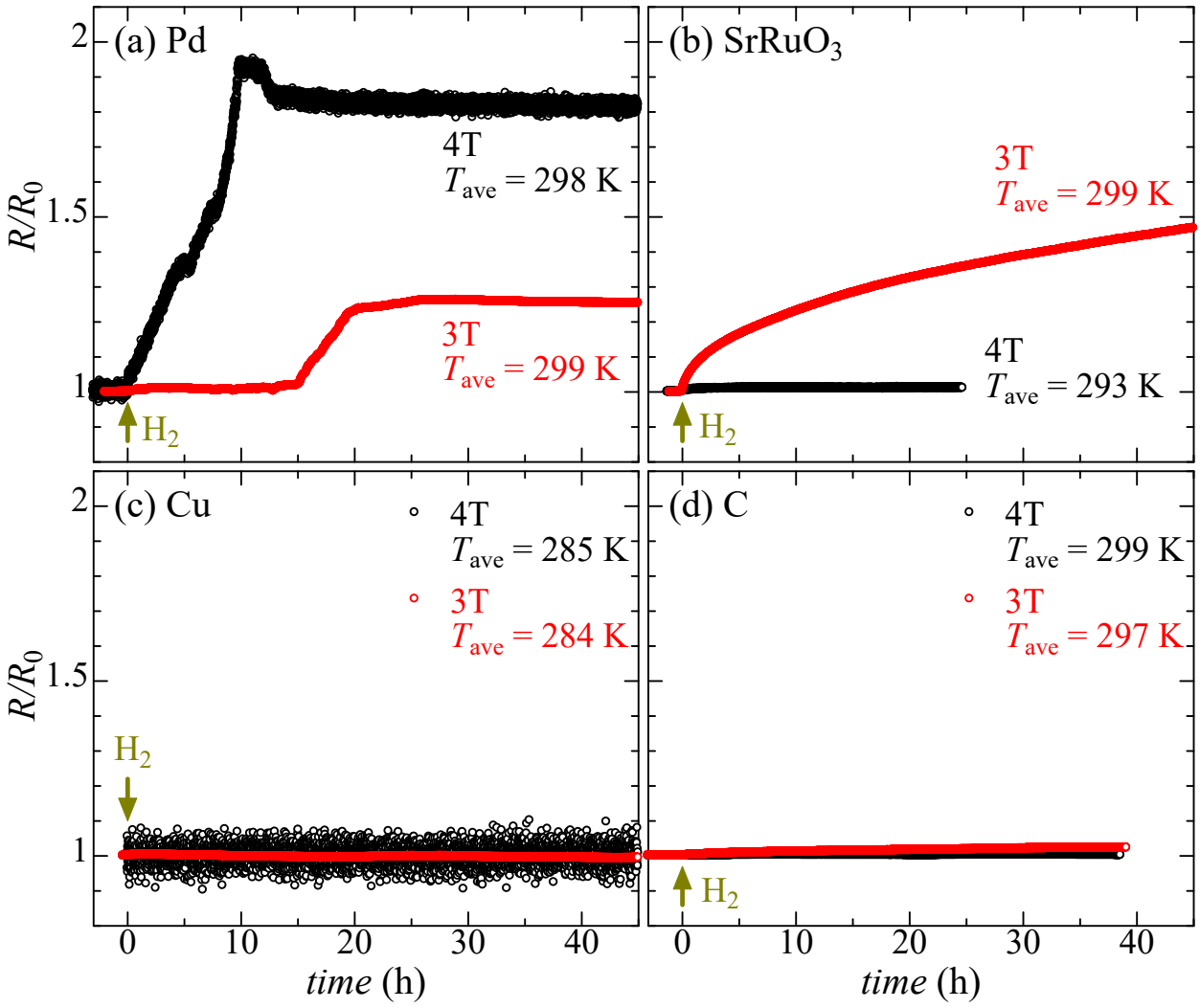

FIG. 3. Normalized resistance $R(t)/R_0$ in H_2 gas atmosphere (3.5×10^4 Pa of H_2 from 0 h) of (a) Pd, (b) $SrRuO_3$, (c) Cu, and (d) Carbon (black: 4T, red: 3T data, respectively) at temperatures $T_{ave}\pm\sim1$ K.

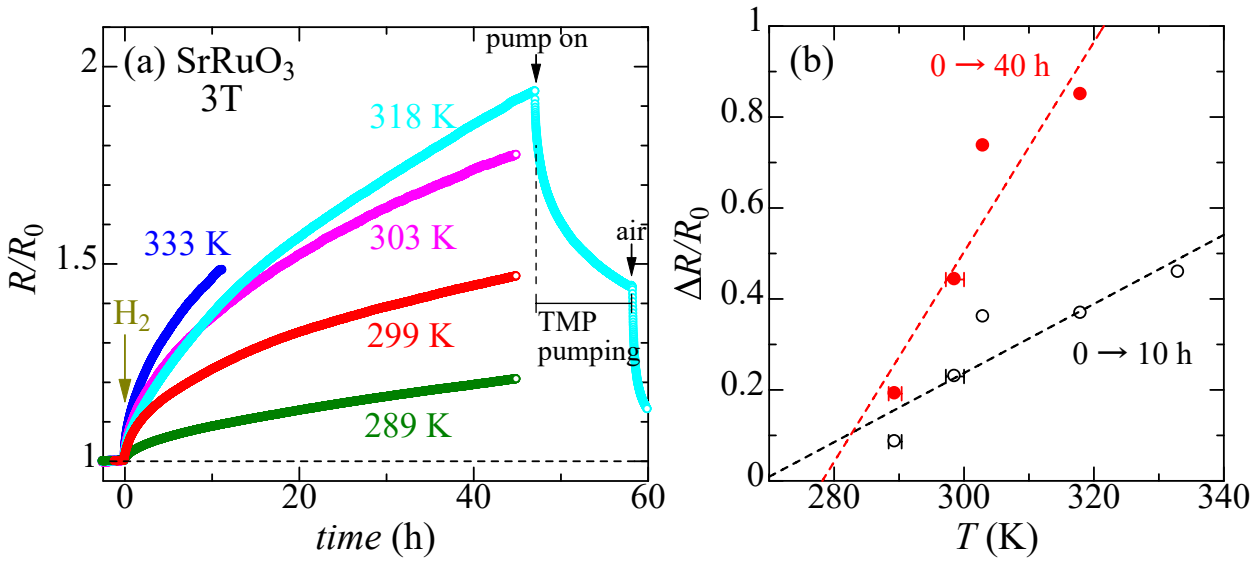

FIG. 4. (a) Temperature dependence of $R(t)/R_0$ for $SrRuO_3$ 3T in H_2 gas atmosphere (3.5×10^4 Pa of H_2 from 0 h). For the 318 K data, the H_2 gas was pumped out from 47 h to 58 h, and then fresh air was introduced at 1 atm at 58 h. (b) $\Delta R(t)/R_0$ versus temperature. $\Delta R(t)/R_0$ is the increase in the normalized resistance from 0 h to t. The data at $t = 10$ h (black open circle) and 40 h (red solid circle) are shown.

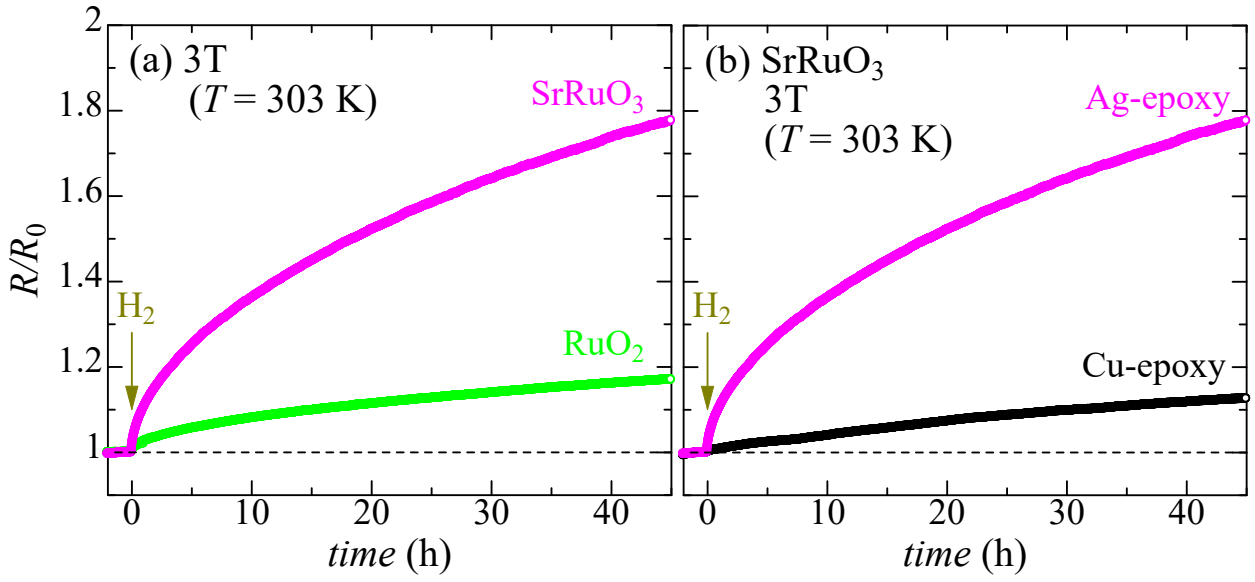

FIG. 5. Comparisons of 3T $R(t)/R_0$ curves for different setups in H_2 gas atmosphere (3.5×10^4 Pa of H_2 from 0 h) at 303 K: (a) $SrRuO_3$ and RuO_2, and (b) Ag-epoxy and Cu-epoxy pad for $SrRuO_3$.

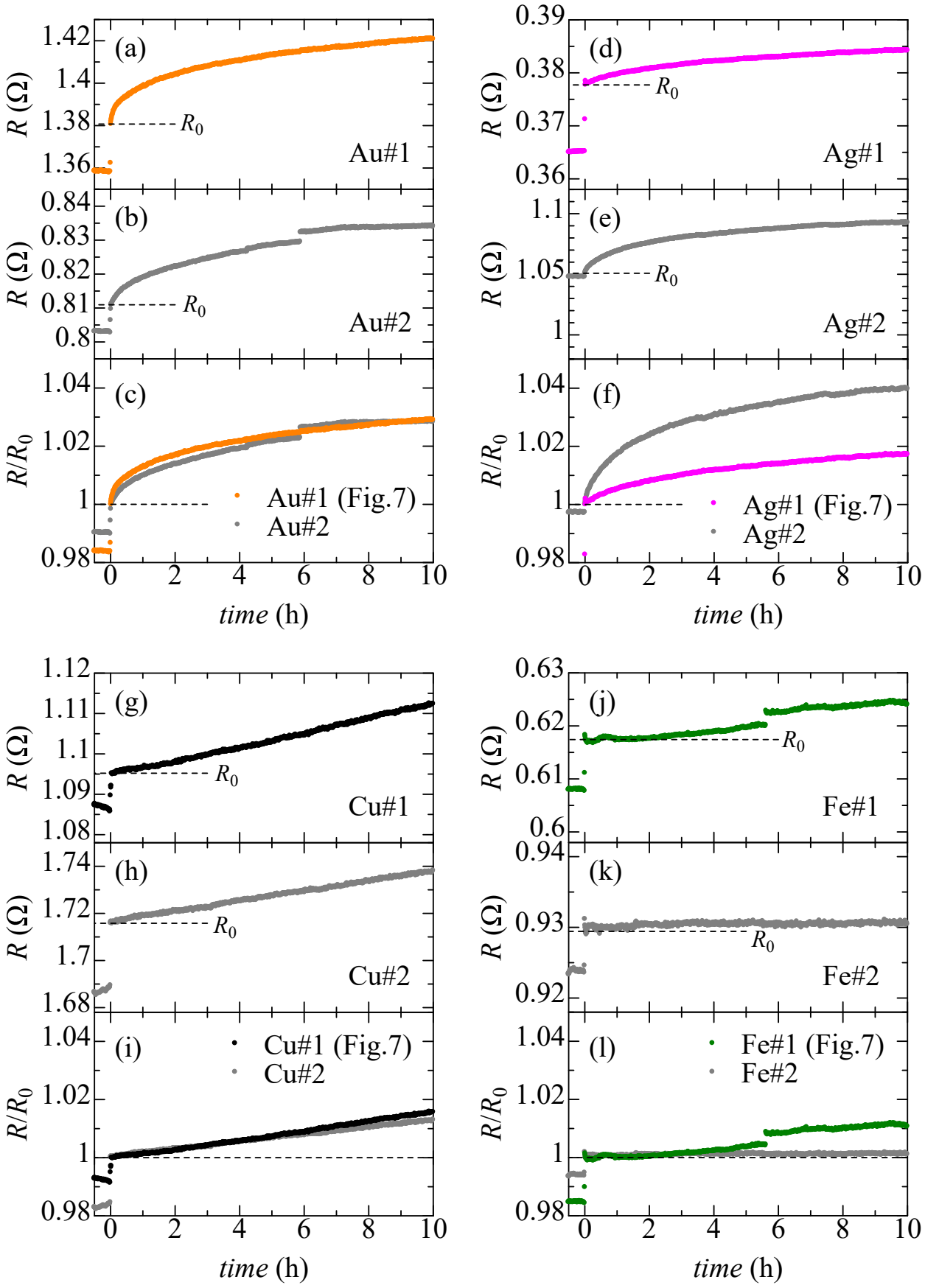

FIG. 6. Resistance $R(t)$ and normalized resistance $R(t)/R_0$ versus time for the $SrRuO_3$-metal tip: (a–c) Au, (d–f) Ag, (g–i) Cu, and (j–l) Fe in H_2 gas atmosphere (3.5×10^4 Pa of H_2 from 0 h) at

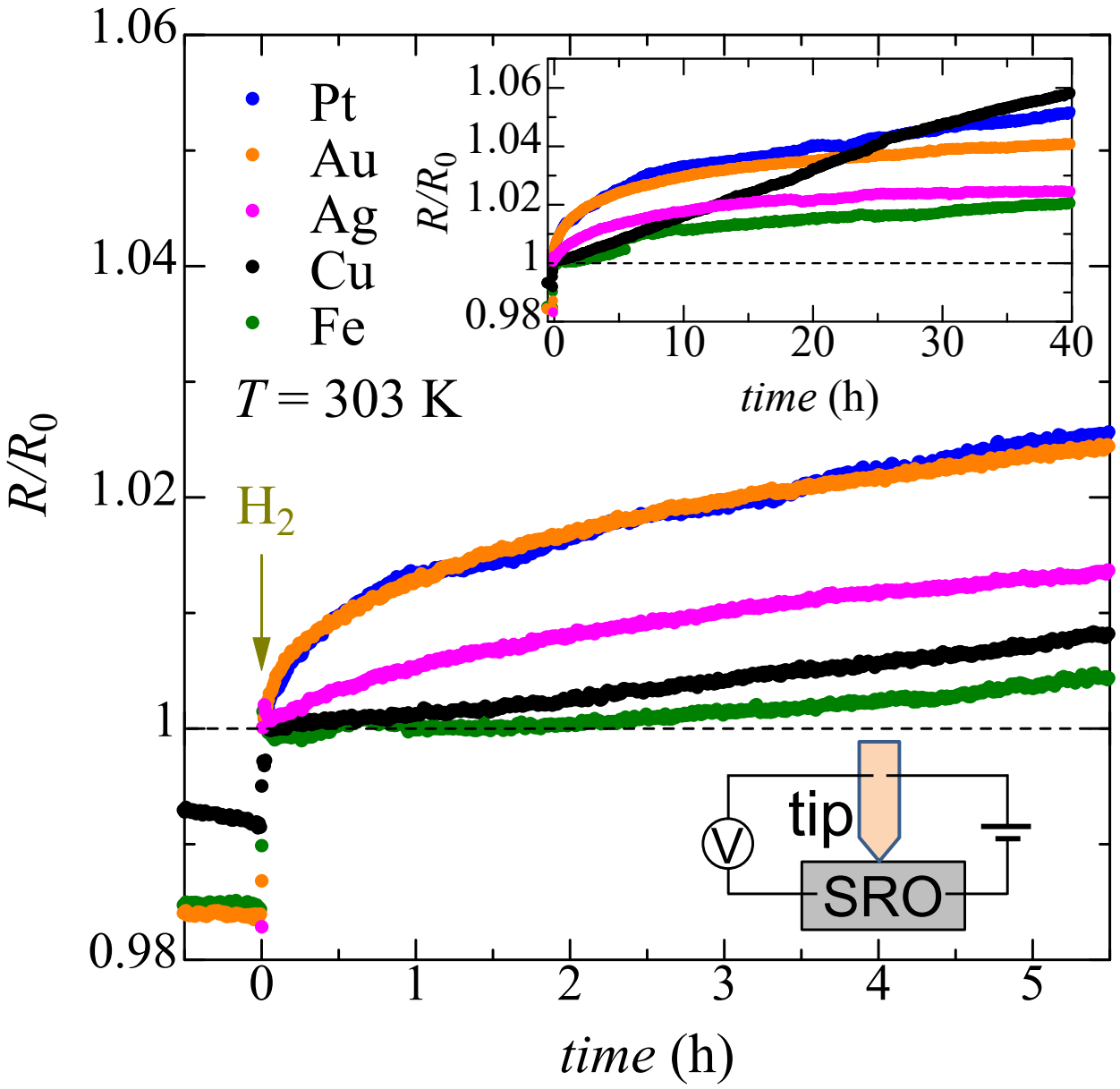

FIG. 7. Tip material dependence of $R(t)/R_0$ for $SrRuO_3$ in H_2 gas atmosphere (3.5×10^4 Pa of H_2 from 0 h) at 303 K obtained using the PC method. Lower inset: schematic of the method. Upper inset: overall measured time scale.

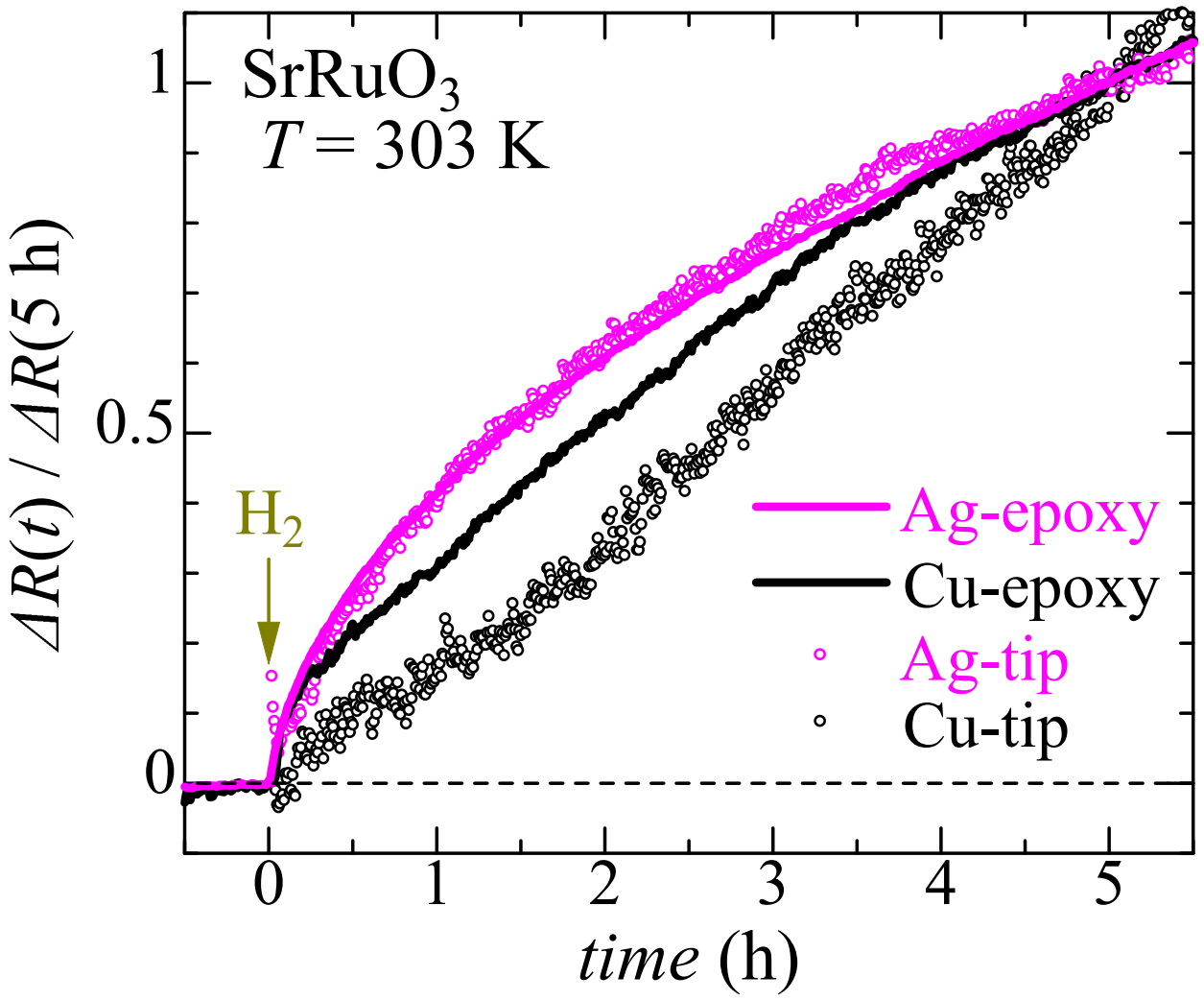

FIG. 8. Comparison of the increase in resistance normalized to that from 0 to 5 h for $SrRuO_3$-Ag and $SrRuO_3$-Cu interfaces obtained by 3T [Fig. 5(b)] and PC (Fig. 7) methods in H_2 gas atmosphere (3.5×10^4 Pa of H_2 from 0 h) at 303 K. $\Delta R(t)$ is the increase in resistance from 0 h to t.

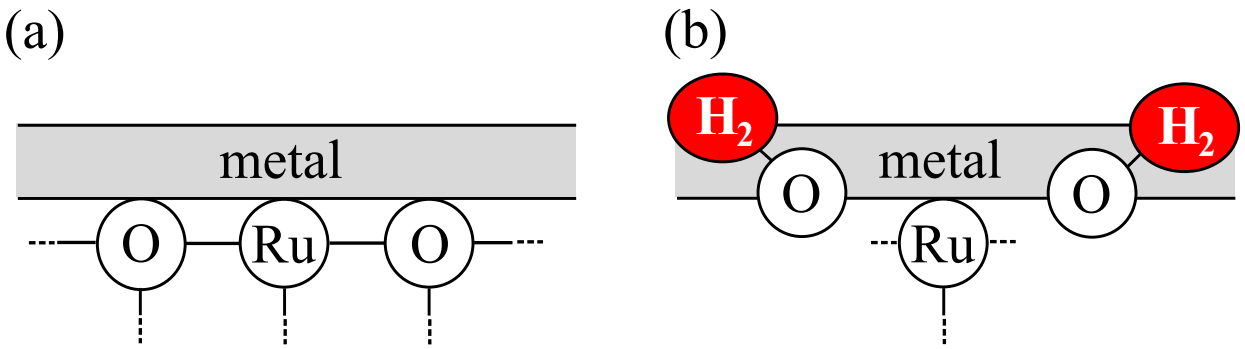

FIG. 9. Schematics of the $SrRuO_3$-metal interface in (a) vacuum and (b) a hydrogen atmosphere. Oxygen atoms at the interface recombine with hydrogen molecules in (b).